Mechanics of Control Element During Irradiation

Massih, A.R.; Isaksson, P.; Ståhle, P.

Published in:
Transactions of the 14th Conference on Structural Mechanics in Reactor Technology

1997

Document Version:
Publisher's PDF, also known as Version of record

SMIRT

SMIRT 14
LYON-FRANCE
August 17-22, 1997

International Association for Structural Mechanics In Reactor Technology

Transactions of the 14th International Conference on

Structural Mechanics In Reactor Technology

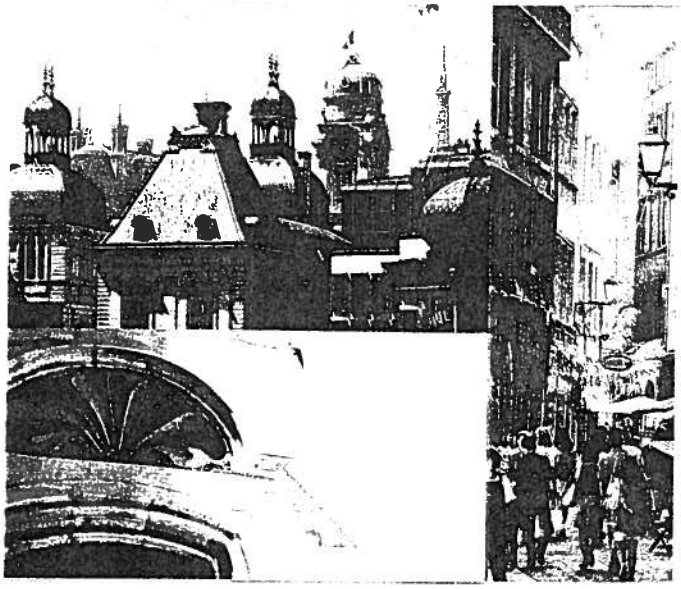

VOLUME 2

Division C

Fuel Element Mechanical Modelling and Core Design

Division D

Life Prediction including Operating Feed-back Experience.
Non Destructive Examination

Commissariat à l'Energie Atomique (CEA) - Electricité de France (EDF) - FRAMATOME
Institut National des Sciences Appliquées de Lyon (INSA)

Transactions of the **14th International Conference on Structural Mechanics in Reactor Technology** (SMiRT 14), Lyon, France, August 17-22, 1997

Mechanics of control element during irradiation

Massih A.R.[1], Isaksson P.[2], Stahle P.[2]
(1) ABB Atom, Sweden
(2) Lulea University of Technology, Sweden

ABSTRACT

A finite element analysis of a control rod blade consisting of B_4C powder and stainless steel cladding has been performed using the ADINA program. An algorithm for finite element calculations of a porous material such as B_4C powder has been developed. This algorithm describes both the swelling and consolidation behavior of B_4C powder. The Gurson yield condition for isotropic porous media with cavities has been utilized to model the consolidation phenomenon. The constitutive model has been implemented in a user-defined subroutine of the ADINA finite element code. A two-dimensional 4-node isoparametric solid element has been used. A Newton-Raphson scheme has been applied to solve the nonlinear finite element equations. The model has been used to predict stresses and strains of the blade during irradiation when both B_4C swelling and irradiation-induced creep of stainless steel are effective.

1 INTRODUCTION

Control rods in boiling water reactors (BWR) have cruciform cross section. Each rod consists of four blades made of stainless steel containing boron carbide neutron absorber material. A typical ABB Atom blade is about 8 mm thick, 125 mm wide, 3.65 m long, and contains 586 holes. The holes are horizontally drilled through the width of the blade. Typically 562 of the holes are filled with natural boron carbide (B_4C) powder, with 0.70 fraction of theoretical density. The remaining holes in the blade's upper part contain hafnium pins. Both boron and hafnium are neutron absorbing materials suitable for BWR applications.

Natural B_4C contains about 20% the isotope ^{10}B which upon neutron absorption produces helium gas. The internal production of helium gas and point defects generated in neutron-irradiated boron carbide causes significant swelling, the size of which is roughly linear with neutron fluency [1, 2]. Nevertheless, some of the produced helium gas can diffuse through the B_4C crystalline to the free surface and get released into the available void volume of the blade. Released helium gas leads to internal pressure buildup in the blade. The swelling of boron carbide, on the other hand, can lead to a mechanical interaction between B_4C powder and stainless steel cladding. This effect is believed to be the main mechanical load causing the stress cracking of the blade.

In this work we have attempted to simulate the swelling of B_4C in the control rod blade and

the mechanical interaction between the B_4C powder and stainless steel; and then we have calculated the stresses induced in the stainless steel blade. An algorithm, based on Gurson's yield criterion [3] for porous materials, has been developed for B_4C powder and implemented in the finite element program ADINA [4].

2 A CONTINUUM MODEL FOR B_4C POWDER

In order to determine the change in relative density of B_4C powder due to plastic deformation we consider the porous material as a continuum having the property of irreversible compressibility. For this purpose a yield criterion for a porous solid is needed. For a ductile material containing a certain volume fraction of spherical voids, Gurson [3] has provided an approximate yield criterion of the form

$$F = \frac{3S_{II}}{k^2} + 2p\cosh\left(\frac{S_I}{2k}\right) - (1+p^2) = 0 \quad , \tag{1}$$

where F is the Gurson plastic potential, k is a shear flow stress, p is the void volume fraction, or porosity, and S_I is the first invariant of the stress tensor and S_{II} is the second invariant of the deviatoric stress tensor:

$$S_I = \sigma_{ii} \qquad S_{II} = \frac{1}{2} S_{ij} S_{ij} \tag{2}$$

with $S_{ij} = \sigma_{ij} - S_I\,\delta_{ij}/3$ being the deviator stress tensor. Here repeated index assumes summation and δ_{ij} is the Kronecker delta. The macroscopic effective von Mises stress is $\sigma_e = \sqrt{3S_{II}}$ and the hydrostatic stress $\sigma_m = S_I / 3$. Using an associated flow rule, the plastic strain increment is given by the normality relation:

$$d\varepsilon_{ij}^{p} = d\lambda \frac{\partial F}{\partial \sigma_{ij}} \quad \begin{cases} d\lambda \geq 0 & \text{if} \quad F = 0 \quad \text{and} \quad dF = 0 \\ d\lambda = 0 & \text{if} \quad F < 0 \quad \text{and} \quad dF < 0 \end{cases} \tag{3}$$

where $d\lambda$ is the multiplier of time-independent plasticity and F is the Gurson potential given by (1). The implication of this model is that the voids are assumed to be randomly distributed, such that the macroscopic properties are isotropic. Furthermore, we note that when p=0, (1) reduces to the von Mises yield condition.

Tvergaard [5] carried out micromechanical studies on porous materials and compared the results with predictions of the yield function (1). Based on this comparison Tvergaard concluded that p' should be scaled by q, i.e., $p' = q\,p$ where q=1.5. Our aim here is to obtain a constitutive law (stress versus strain) for the material under consideration. In a previous paper [6] we obtained this relation for the Drucker-Prager yield condition [7]. It is noted that, the yield surface dependence of the Drucker-Prager law is a linear function of the hydrostatic tension. Substituting for F, from (1), in (3) gives:

$$d\varepsilon_{ij}^{p} = d\lambda\left[\frac{3}{k^2} S_{ij} + p\frac{\delta_{ij}}{k}\sinh\left(\frac{S_I}{2k}\right)\right] \tag{4}$$

and

$$d\varepsilon_{ii}^{p} = d\lambda\left[\frac{3p}{k}\sinh\left(\frac{S_I}{2k}\right)\right] \tag{5}$$

Equation (6) shows that an increase in volume always accompanies plastic deformation, a characteristic of porous material. In the Gurson model this change in volume depends nonlinearly on the hydrostatic tension (cf. the Drucker-Prager law which gives $d\varepsilon_{ii}^{p} = d\lambda\alpha$). It is observed from (5) that when $S_I > 0$, the Gurson solid swells, while for $S_I < 0$ it consolidates.

The plasticity multiplier can be derived by a procedure described in [6]. It is expressed by:

$$d\lambda = \frac{k^2}{6G}\left[2G\frac{\sqrt{\hat{e}_{II}}}{\sqrt{S_{II}}} - 1\right] \tag{6}$$

where $\hat{e}_{II} = \hat{e}_{ij}\hat{e}_{ij}/2$, $\hat{e}_{ij} = {}^{t}e_{ij}^{e} + de_{ij}$, $\hat{e}_{ij} = \varepsilon_{ij} - \varepsilon_{kk}\delta_{ij}/3$ is the elastic deviator tensor, $G = E/[2(1+\nu)]$, E is Young's modulus and ν is Poisson's ratio.

The swelling rate of B_4C in a reactor is neutron fluence dependent (see section 4), hence the swelling strain increment tensor is described by

$$d\varepsilon_{ij}^{s} = \delta_{ij}\Phi dt \tag{7}$$

where we assumed that the swelling is a linear function of time and Φ denotes the swelling rate. The effective stress for the Grurson model is during yielding expressed by

$$\sigma_e = k\left[(1+p^2) - 2p\cosh\left(\frac{S_I}{2k}\right)\right]^{1/2} \tag{8}$$

According to Hooke's law we readily obtain

$$\sigma_{kk} = 3K\left[\hat{\varepsilon} - d\varepsilon_{kk}^{p} - d\varepsilon_{kk}^{s}\right] \tag{9}$$

where $K = E/[3(1-2\nu)]$ and $\hat{\varepsilon} = {}^{t}\varepsilon_{kk}^{e} + d\varepsilon_{kk}$. Now substituting for $d\varepsilon_{kk}^{p}$ and $d\varepsilon_{kk}^{s}$ from (6), (7) and (8), respectively, we obtain

$$\sigma_{kk} = S_I = 3K\left\{\hat{\varepsilon} - \frac{3pk}{6G}\left[2G\sqrt{\frac{\hat{e}_{II}}{S_{II}}} - 1\right]\sinh\left(\frac{S_I}{2k}\right) - 3\Phi dt\right\} \tag{10}$$

From (11), $\sigma_e = \sqrt{3S_{II}}$ can be derived

$$\sigma_e = \frac{2pG\sinh\left(\frac{S_I}{2k}\right)\sqrt{3\hat{e}_{II}}}{p\sinh\left(\frac{S_I}{2k}\right) - \frac{2G}{k}\left[\frac{S_I}{3K} - \hat{\varepsilon} + 3\Phi dt\right]} \tag{11}$$

Equations (10) and (11) can be solved simultaneously to determine σ_e and S_I (e.g. by an iterative method).

3 THE FINITE ELEMENT METHOD

The finite element computations have been carried out with the aid of the ADINA computer program [4]. The Gurson law described in the preceding section has been implemented in ADINA's special user-defined subroutines. A two-dimensional solid material element has been selected for the subroutine. We have used a 4-node isoparametric element with two degrees of freedom, i.e., x- and y-directions. A Newton-Raphson iteration scheme for the solution of nonlinear finite element equations has been employed. The governing equations are

$$\mathbf{KU}=\mathbf{R} \quad , \tag{12}$$

where $\mathbf{K}$ is the stiffness matrix, $\mathbf{U}$ is the vector of nodal displacement variables, and $\mathbf{R}$ is the load vector representing the driving forces including the body and surface forces. The gradient of (12) can be expressed by

$$\Delta \mathbf{U}^{t} \frac{\partial}{\partial \mathbf{U}}(\mathbf{KU})\Big|_{\mathbf{U}={}^{t+\gamma\Delta t}\mathbf{U}^{(i-1)}} = {}^{t+\gamma\Delta t}\mathbf{R} - {}^{t+\gamma\Delta t}(\mathbf{KU})^{(i-1)} \tag{13}$$

and

$${}^{t+\gamma\Delta t}\mathbf{U}^{(i)} = {}^{t+\gamma\Delta t}\mathbf{U}^{(i-1)} + \Delta \mathbf{U}^{(i)} \tag{14}$$

where $1/2 \le \gamma \le 1$. The index i denotes the iteration number and the vector $\Delta \mathbf{U}^{(i)}$ represents the increment in the solution variable at iteration i. Hence one obtains a linear system of algebraic equations which must be solved at each equilibrium iteration.

We have used ADINA's procedures to solve the elastoplasticity constitutive equation for stainless steel during irradiation and the interaction of stainless steel blade with boron carbide. The theory of these procedures used in ADINA is the classical incremental theory of plasticity based on the Prantl-Reuss equations details of which are described in [4, 8] and hence are not repeated here. We only mention that the von Mises yield criterion and associated flow rule where the plastic volumetric strains are zero is assumed for stainless steel.

4 IN-REACTOR BEHAVIOR OF B_4C AND STAINLESS STEEL IN CONTROL ROD ELEMENT

During in-reactor operation of control rod element the ^{10}B isotope in B_4C (natural boron consist of about 20% of the isotope ^{10}B) reacts with neutron according to: $^{10}B + n \rightarrow {}^{7}Li + He$ where ^{7}Li is preferentially left in an excited state with energy 0.48 MeV [9]. The produced helium gas [1, 2] forms bubbles inside B_4C crystal grains which in turn leads to gaseous swelling. Fuhrman [10] has measured the volume displaced by the irradiated B_4C powder particles, excluding the interparticle void volume that existed within boron carbide. The control element studied by Fuhrman had a tubular stainless steel (Type 304) cladding. The B_4C powder had a density of about 0.70 of theoretical density. The results of Fuhrman's measurements, volumetric swelling ratio versus $\%\,^{10}B$ depletion are depicted in Fig. 1. As can be seen from this figure B_4C particles have swelled around 30% at an estimated ^{10}B depletion of 30%. The corresponding measurements of the diameter of the stainless steel tube showed, however, that the tensile strain was about 0.2%. This implies that the boron carbide swelling was accommodated within the interparticle voids of the powder. Similarly measurements by Eikelpasch et al., see ref [11] showed that a B_4C swelling of 16% at 53% ^{10}B depletion resulted in a hoop tensile strain of 0.2%. The ultimate goal of the constitutive theory for the system under consideration is to predict and explain this effect.

5 COMPUTATIONS

The models presented in Sections 2 to 4 are used to calculate the mechanical behavior of an ABB Atom control rod blade during irradiation. We have attempted to compute the stress induced in the stainless steel blade during irradiation when both B_4C consolidation and swelling is effective. Creep effects have been found to be negligible [6] and is hence not considered in the present study. First in Section 5.1 we describe the geometry of the considered structure.

Table 1. Dimensions and material properties of an ABB control rod.

Blade thickness, mm	8.05	
Hole diameter, mm	5.4	
Depth of the holes, mm	112	
Number of holes with B_4C	562	
Minimum outer wall thickness, mm	0.92	(nominal, 1.325)
Minimum hole ligament, mm	0.5	(nominal, 0.8)
Length of control rod blade, mm	3650	

Stainless steel at T=300° C:		**Boron carbide at T=300° C:**	
Modulus of elasticity, *E*, MPa	195000	Modulus of elasticity, *E*, MPa	191000
Poisson's ratio, ν	0.3	Poisson's ratio, ν	0.18
		Yield strength irradiated, MPa	10

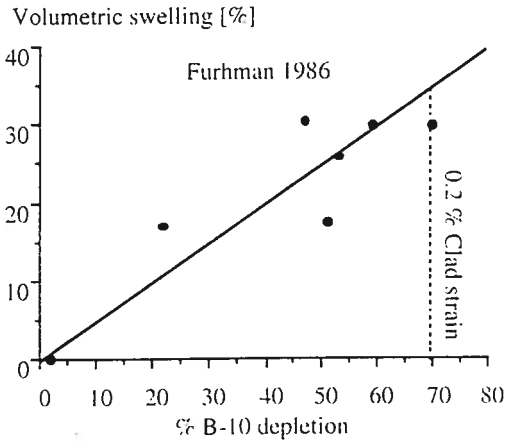

Fig. 1.Fuhrman's volumetric B_4C swelling as a function of ^{10}B depletion during reactor operation.

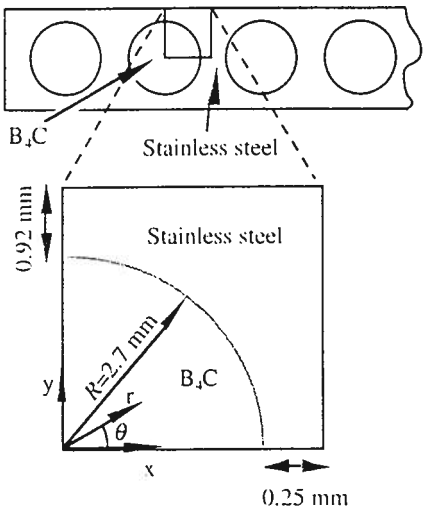

Fig 2. A schematic of a portion of a control rod blade (see also table 1).

5.1 Geometry

The ABB control rod blade is about 8 mm thick, 125 mm wide, 3.65 m long and contains 562 horizontally drilled holes filled with boron carbide. Typical dimensions for the structure and pertinent material data at 300 °C are listed in Table 1. In Fig 2 the cross section geometry of a portion of the ABB control rod blade is displayed. The symmetry of the blade allows us to model only a quarter of a cell containing a B_4C filled hole with stainless steel cladding. A periodic boundary condition is assumed in order to cover the entire blade structure.

5.2 Finite element model

In the FE model a 4-node isoparametric element with two degrees of freedom, translations in x- and y-directions are used. The finite element mesh for the simulation is shown in Fig 3 which consists of about 1200 elements. The coordinates of the FE model are defined in Fig 4. The four edges A, B, C and D are subjected to the boundary conditions which are also shown in Fig 4. The shear traction, τ_{xy} is taken to be zero along all the edges and the normal traction is zero only along edge A, which is the only traction free surface in the model. The displacements u, v are in the x- and y-direction, respectively. To preserve vertical compatibility at the edge B the nodes are constrained to a straight vertical line between the two corners. Symmetry conditions are imposed along the edges C and D.

Two-dimensional contact model in ADINA under plain strain conditions without friction is utilized. The option Algorithm 1 [4] is selected for the present analysis. The Algorithm 1 in ADINA uses constraint functions to enforce all the contact conditions at the contact nodes.

The swelling in the z-direction is small compare to the swelling in the x- and y-directions. Therefore, plane strain conditions are assumed in the model and both the stainless steel and the boron carbide are supposed to behave as nonlinear materials. The force transmission from the swelling boron carbide to the stainless steel can only occur in the r-direction. This is because the displacements in the θ-direction along the boron carbide/steel interface at $r=R$ are assumed

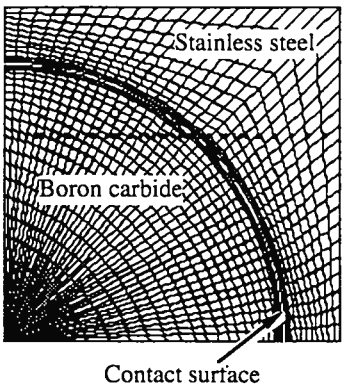

Fig 3. The finite element mesh covering a quarter of a cross-section of the blade comprising an absorber cell boron carbide.

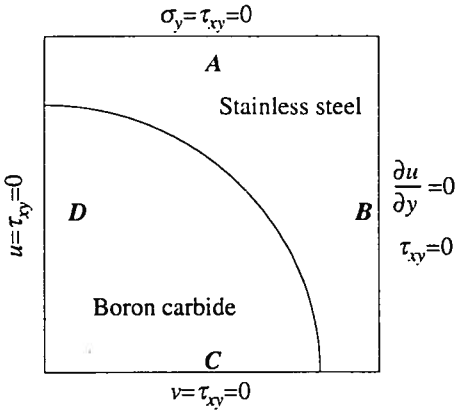

Fig 4. Boundary conditions imposed.

to occur without friction. Let $\Delta u_r = u_r^b - u_r^s$ where u_r^b and u_r^s are the displacements in the radial direction for B_4C and stainless steel, respectively. The contact condition predicts that $\Delta u_r \leq 0$. Similarly, let $\Delta u_\theta = u_\theta^s - u_\theta^b$, i.e., Δu_θ is the change in the displacements in the θ direction across the boron carbide/steel interface.

5.3 Irradiation-induced swelling of B_4C and blade deformation

In this section we present the results of ADINA computations for predicting stresses and strains induced in the stainless steel blade during irradiation as a function of time. Computations take into account the irradiation-induced swelling of B_4C. The irradiation hardening effect of stainless steel on yields strength is also taken into account. We have carried out the calculations for two values of the void volume fraction 0 and 30%, i.e., the p parameter, p=0 and p=0.30 are used. The yield stress for irradiated B_4C is taken to be 10 MPa and the fast neutron flux (≥1 MeV) is assumed to be constant at 2.5×10^{21} n/m^{2}h. The stresses induced in the B_4C as a function time are plotted in Figs 5 and 6. The data are taken from the element which first becomes plastic. It is seen that the case of p=0.30 reduces the effective stress by about 60% after 1,300 hours of irradiation. In Fig. 5 one observes a decreased shear stress and also that the deviation between the two normal stresses is significantly reduced for p = 0.3. This is interesting since it reduces the risc of damage on the B_4C and hence it also delays the introduction of large stresses in the stainless steel.

The plastic deformation begins in the interior of the boron carbide for p=0.30, whereas this occurs in the vicinity of the carbide/steel interface for p=0. The same observation was also made for the Drucker-Prager model (cf. [6]). The observation is interesting because of the consequences the position of the maximum effective stress may have on subsequent development of damage or crack growth which have been observed in real structures. Damage and cracks in the B_4C can be detrimental to the integrity of the stainless steel because of the concentration of stress that results.

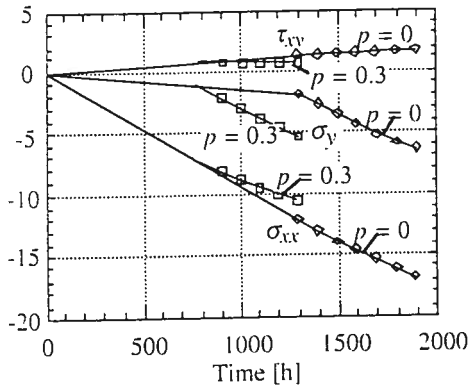

Fig 5. Stress components in B_4C at the element which first becomes plastic.

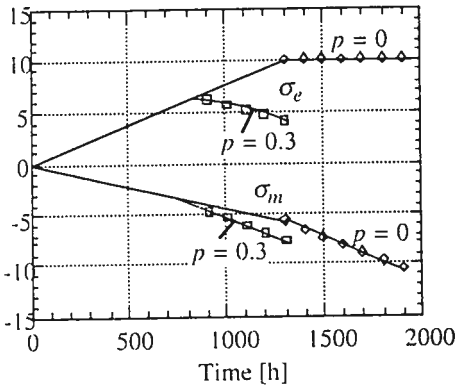

Fig. 6. Effective stress σ_e and hydrostatic stress σ_m in B_4C at the element which first becomes plastic.

6 CONCLUDING REMARKS

The mechanical properties of powder boron carbide neutron absorber material has been modeled using the Gurson constitutive law to account for the effect of consolidation under loads induced by the interaction of B_4C with the stainless steel cladding. The source of the load is the swelling of boron carbide during irradiation. An algorithm for this model has been implemented in a user defined subroutine of the ADINA finite element program. The model has been verified with analytical solutions for a simple geometry. Further it is used to simulate the control rod blade mechanical behavior during irradiation, specially the irradiation-induced swelling of B_4C and creep of stainless steel.

Acknowledgments: We are thankful to Anette Medin for graphic assistance.

References

1. Hollenberg, G.W., B. Mastel & J.A. Basmagian 1980. Effect of irradiation temperature on the growth of helium bubbles in boron carbide.
Journal of American Ceramic Society 63: 376-380.

2. Jostons, A., C.K.H. du Bose, G.L. Copland & J.O. Stiegler 1973. Defect structure of neutron irradiated boron carbide.
Journal of Nuclear Materials 49: 136-150.

3. Gurson, A.L. 1977. Continuum theory of ductile rupture by void nucleation and growth: Part I - yield criteria and flow rules for porous ductile media 1977.
Journal of Engineering Materials and Technology 99: 2-15.

4. *ADINA Theory and Modelling Guide* 1995. ADINA R&D Inc. Watertown, MA 02172, USA.

5. Tvergaard, V. 1982. On localization in ductile materials containing spherical voids.
International Journal of Fracture 18: 237-252.

6. Massih, A.R., P. Isaksson & P. Ståhle 1996. Modelling the behavior of a control element blade during irradiation. To appear in *Computers & Structures.*

7. Drucker, D.C. & W. Prager 1952. Soil mechanics and plastic analysis or limit design.
Quarterly of Applied Mathematics 10: 157-165.

8. Bathe, K-J. 1996. *Finite Element Procedures.*
Prentice Hall, Engelwood Cliffs, N.J.

9. Krane, K.S. 1988. *Introductory Nuclear Physics*, chap 12.
John Wiley & Sons, New York.

10. Fuhrman, N. 1986. Behavior of irradiated B_4C.
Electric Power Research Institute Report NP-4533-LD, Palo Alto, California.

11. Strasser, A. & W. Yario 1981. Control rod materials and burnable poisons.
Electric Power Research Institute Report NP-1974, Palo Alto, California.